Supplement of Nat. Hazards Earth Syst. Sci., 26, 299–314, 2026
https://doi.org/10.5194/nhess-26-299-2026-supplement

Natural Hazards and Earth System Sciences
Open Access
EGU

Supplement of

The first Earthquake Early Warning System for the high-speed railway in Italy: enhancing rapidness and operational efficiency during seismic events

Simona Colombelli et al.

Correspondence to: Simona Colombelli (simona.colombelli@unina.it)

S1. Preliminary site characterization and permanent station installation.

During the preliminary phase of the project implementation, surveys were conducted at each RFI site (referred to as Technological Points, hereinafter PT) to select the optimal station positioning, to inspect the overall site conditions and to install temporary stations for about one week in each site. In each PT, data were recorded continuously for about 1 week, after the installation of a temporary accelerometric station. Specifically, in each site two accelerometric seismic sensors were installed: one outside the building, and the other inside the building, positioned into a dedicated well. The distance between the sensors was about 15 m.

The preliminary analyses allowed to: study the characteristics of the noise level at each recording site; evaluate their quality with respect to the reference levels (Peterson, 1993); identify the most common sources of noise (such as the presence of current generators nearby some sites) and evaluate their effect on the EW software operations. Noise measurements were carried out to investigate both natural and anthropic noise sources (e.g., noise produced by the train passages, vibrations produced by adjacent structures, TLC antennas, high voltage systems, etc.) produced directly or indirectly by the railway line system and which could interfere with seismic signals.

Data acquired though the temporary stations were used to perform a preliminary site characterization using time and frequency domain analyses. As for time domain analyses, we performed: 24 h continuous daily monitoring and visual inspection of recorded signals; measurement of the signal Peak Ground Acceleration (PGA) and Peak Ground Velocity (PGV), measurement of the signal Root Mean Square Acceleration (ARMS) and Velocity (VRMS). As for frequency domain analyses, these included: Power Spectral Density (PSD) computation, spectrogram analysis and spectral ratios of the horizontal to vertical components (H/V). Figure S1 shows examples of PGA, PGV, ARMS, VRMS and the related histogram distributions as obtained for a single PT. The histograms show the presence of two peaks in the distributions, which are associated to the train passage (the peak corresponding to the highest amplitude values) and to the reference noise level (the lowest amplitude level). Figure S2 shows an example of Power Spectral density analyses. After the preliminary site characterization, permanent stations were installed at each site by an Italian equipe of specialized technicians, who performed surface wells and installed the sensors. The same equipe also performed boreholes and was in charge of the installation of sensors in depth.

S2. Performance on scenario earthquakes

The occurrence of an earthquake that produces dangerous shaking along the route and for which the system does not properly react – a missed alert, de facto – is a crucial aspect of an early warning system and deserves further comments. To validate the trigger criteria, we considered a catalogue of historical earthquakes (CPTI15; Rovida et al 2020) that occurred in Italy between 1000 and 2020 (same catalogue as used for the performance analysis already presented in the main text) and extracted, from this catalogue, the events with an predicted PGA value larger than 10 %g, at least in one point on the railway. The predicted PGA is obtained with the Italian GMPE from Bindi et al. (2011).

We simulated the criteria for the first alert release that is embedded in the *SSR2* configuration of the Decision Module. This requires the predicted $PGA_{pred} > 10$ %g at one station and $PGA_{pred} > 5$ %g at the two adjacent stations and represents the alert criteria currently adopted by the operational EEW system running on the Italian high-speed railway.

We evaluated the expected shaking produced by these earthquakes along the route and whether they would or would not have triggered the activation of the EEW system. The results are shown in Figure S9. The system performed as expected in all the selected scenario, indeed, all the earthquakes would have triggered the activation of the alert, resulting in the interruption of train circulation on a portion of the line (ASR, Alerted Segment of the Railway).

The results confirm that the alert criteria currently implemented in the Decision Module is adequate to respond to the occurrence of significant earthquakes nearby the railway line. Moreover, for these scenario examples the predicted ASR ranged from 20 to 50 km, allowing the closure of only a partial segment of the line, while keeping the circulation possible in the rest of the route.

It is important to note that, in this simulation, we did not include the aleatory variability of the predicted PGA associated with the empirical relations between P-wave peak velocity, acceleration, and displacement amplitudes. Since this analysis relies entirely on PGA values predicted through empirical GMPEs (for a given location and magnitude in the catalogue), we do not make any consideration of the other steps of the EWS—such as P-wave picking, train/earthquake discrimination, or waveform quality control—that are normally carried out in real time.

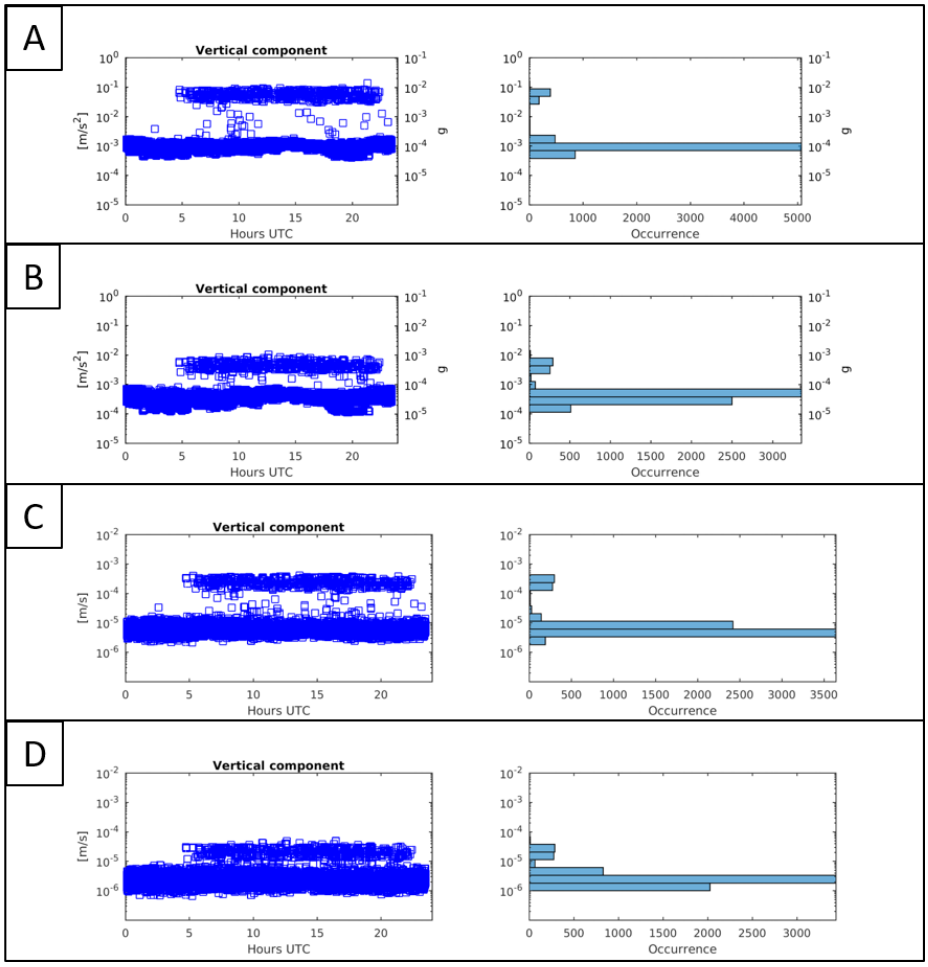

Fig. S1.

Preliminary Time domain analyses. Left panels show the results of analyses over a period of 24 hours for 5 days. Right side are the related histogram distributions. Panel a): PGA of the vertical component of recorded waveforms; Panel b) Root Mean Square of Acceleration (ARMS) of the vertical component; Panel c) PGV of the vertical component; Panel d) Root Mean Square of Velocity signals on the vertical component.

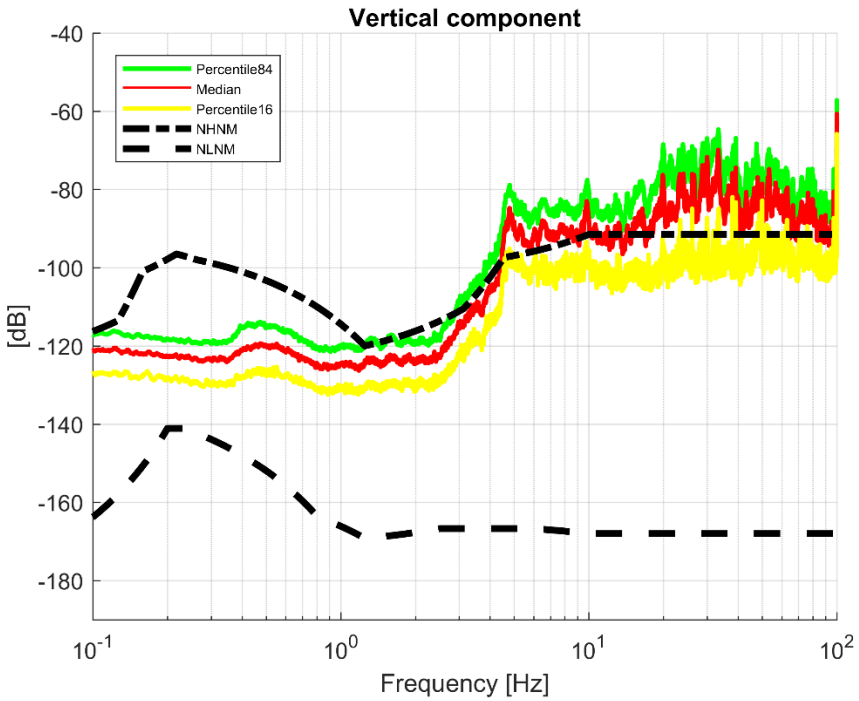

Fig. S2.

Power Spectral Density. The figure shows an example of typical Power Spectral density representation. The dotted lines are the NHNM (i.e. New High Noise Model) and the NLNM (i.e. New Low Noise Model) as extracted from Peterson (1993). The red curve is the median PSD, while the green and yellow lines are the 84 and 16 percentiles, respectively.

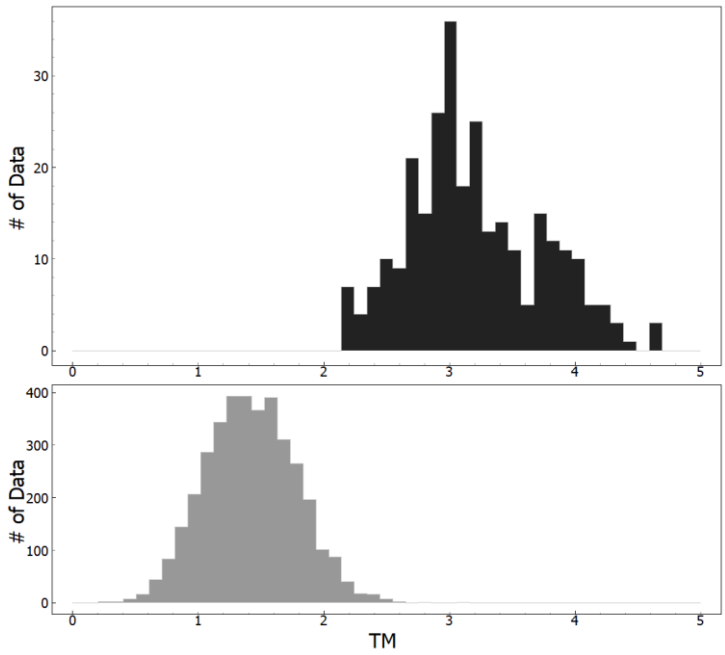

Fig. S3.

Train Marker distribution. The figure shows the TM parameter distribution for trains (top, black histograms) and earthquakes (grea, bottom histograms).

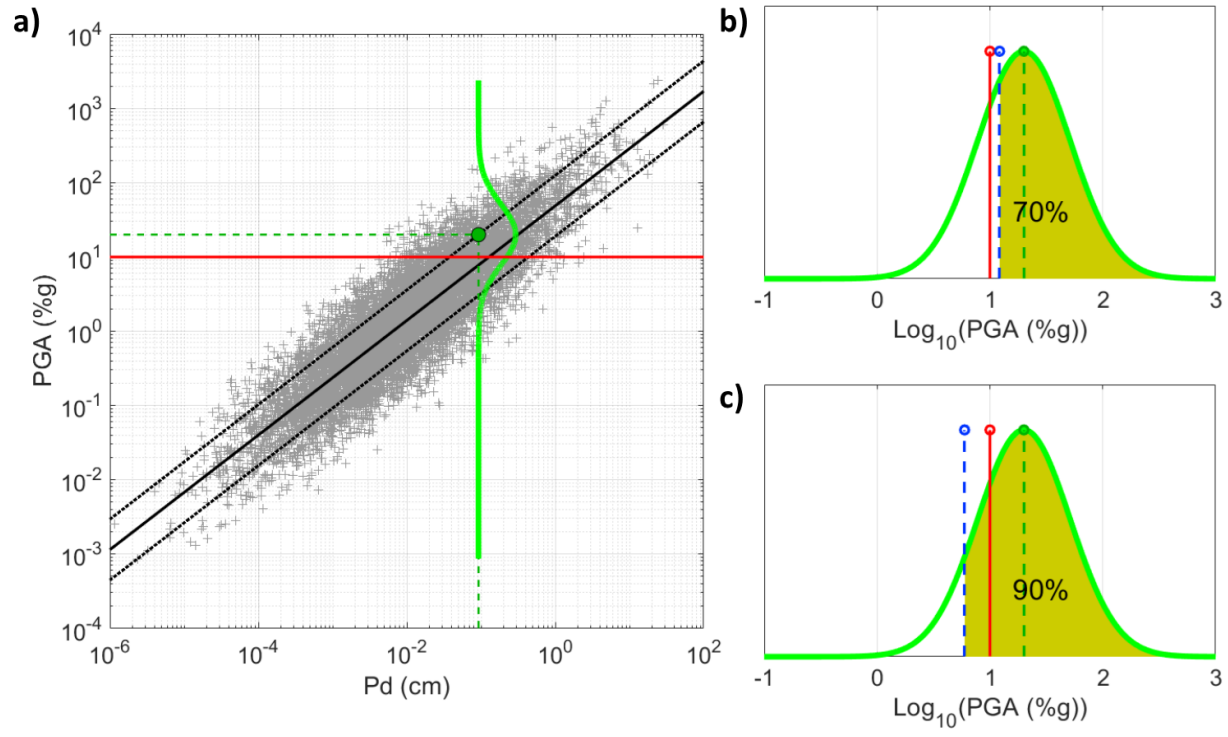

Fig. S4.

Probabilistic decision scheme for alert declaration. a) Empirical relation between P_d and PGA (shown as a solid black line) and data distribution (gray dots). The black dashed lines refer to the ±σ confidence bounds. The horizontal, red solid line is the PGA threshold (PGA^{th}). When a certain P_d value is measured (vertical green dashed line), we predict the PGA following the +σ level (green circle) with an uncertainty Gaussian distribution given by the green, solid line. For simplicity, we report only one relation, but similar considerations can be done for each empirical relationship. In panels b) and c), we show two examples of the operating decision module. In both cases, the same predicted *log(PGA)* value (green circle) is obtained with the same uncertainty Gaussian distribution (green, solid line) and the same alerting threshold, $log(PGA^{th})$ (red vertical line). In the first example (panel b), we set EPL=70% (yellow area). In this case, the predicted *log(PGA)* including the exceedance value (blue dashed line) is greater than the threshold and thus the system declares the alert. In panel c), EPL=90%, and the alert is not issued.

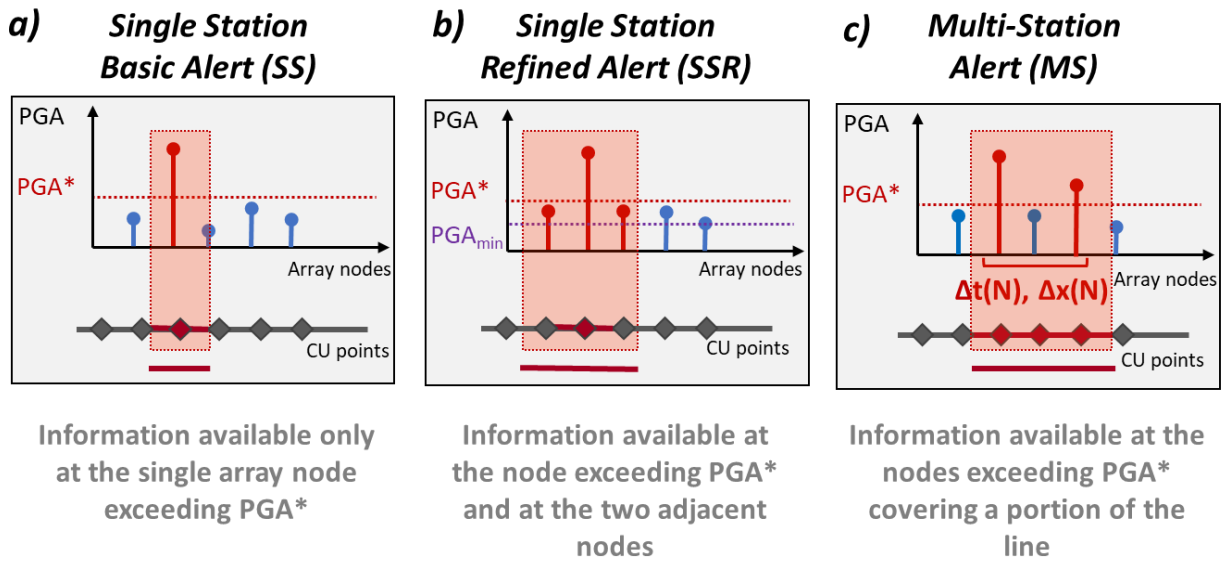

Fig. S5.

Decision Module configurations for the first alert release. The conceptual sketch shows the configurations adopted for the first alert release, going from the simplest Single Station Basic (SSB) (panel a) configuration to the more sophisticated Multi Station Alert (MSA) (panel c). For each panel, the sketch shows the condition for alert release, related to the exceedance of one or more nodes of the PGA threshold. The bottom gray line in each panel shows the segment of line (in red) where the system indicates that operational restrictions are recommended.

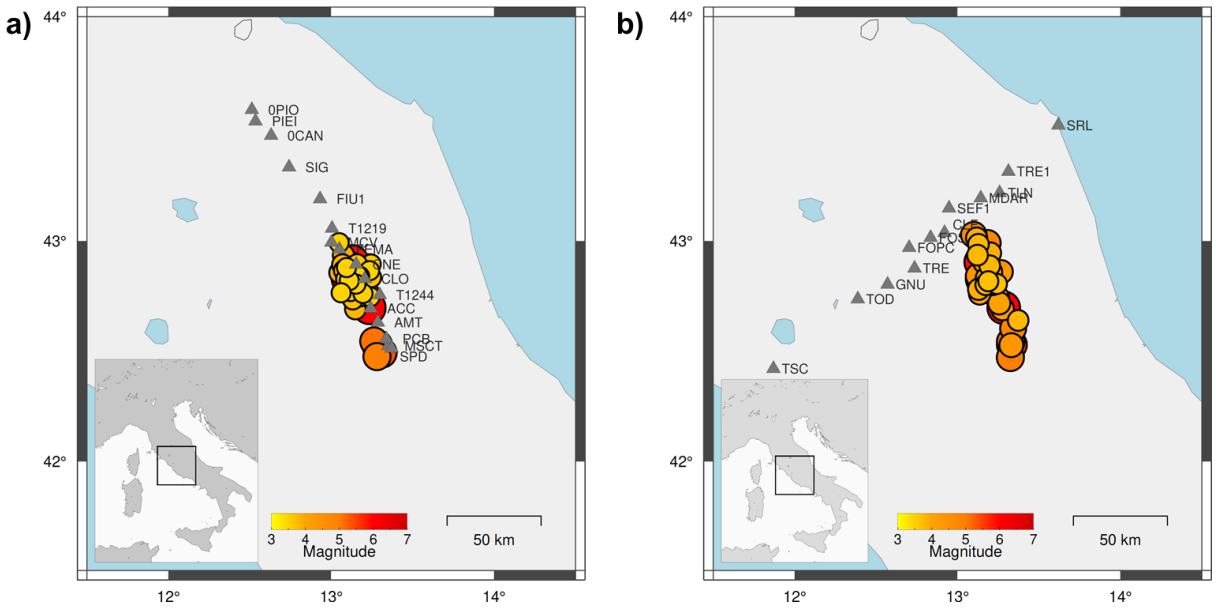

Fig. S6.

Dataset. The figure shows the two networks used for the simulations, with the stations used (gray triangles) and the epicentral positions of the events (circles). Panel a) shows the Apennine Array, while panel b) shows the Anti-Apennine Array. In both panels, circles are colored according to the event magnitude, the size of the circles is proportional to the event magnitudeand the depth of the events varies between 8 and 11 km.

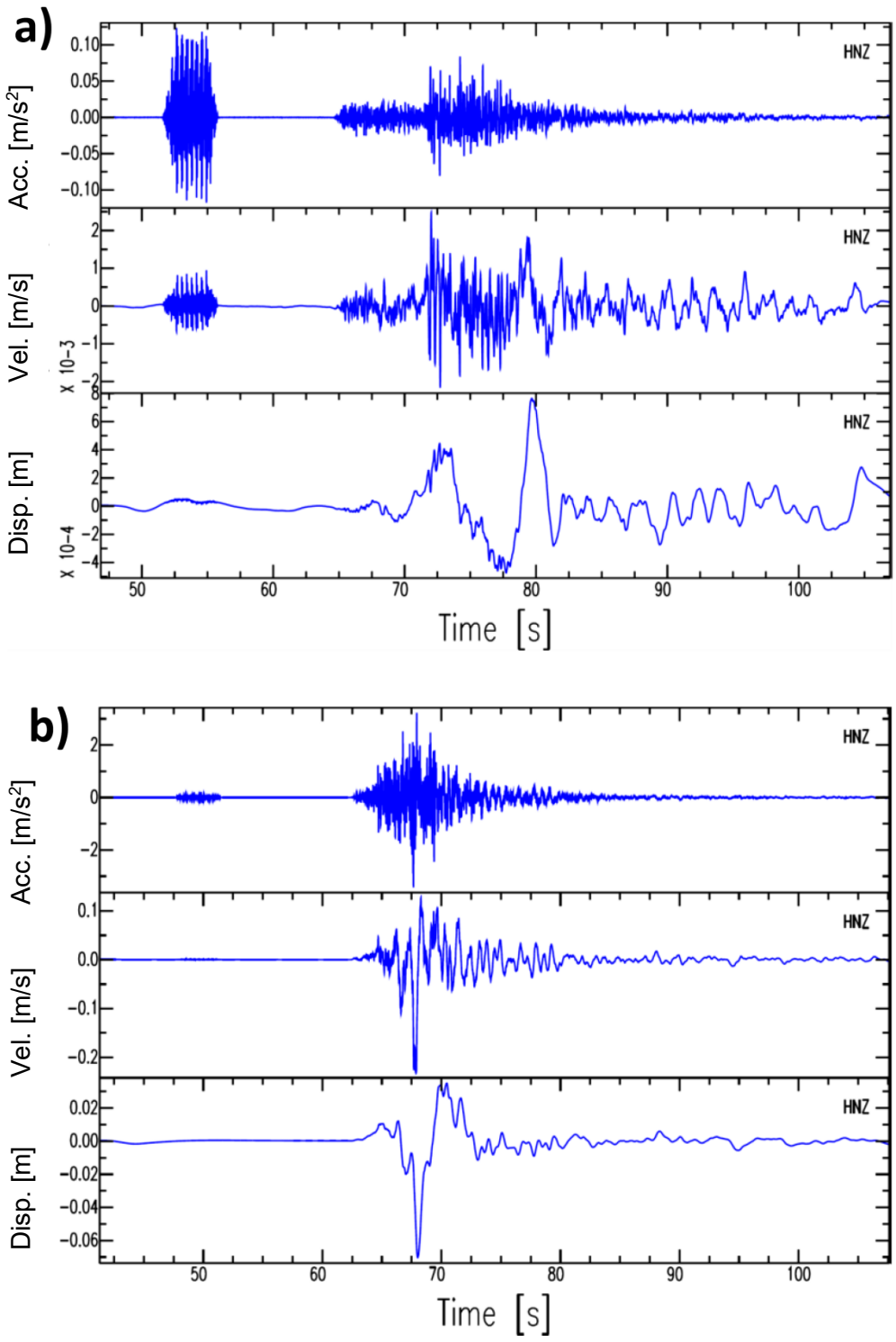

Fig. S7.

Example of waveform and train passage. The figure shows the superimposition of a train transit signal just before the occurrence of a M 5.4 earthquake (panel a) and for a M6.5 earthquake (panel b). From top to bottom, the signals in acceleration, velocity and displacement are shown.

a)

b)

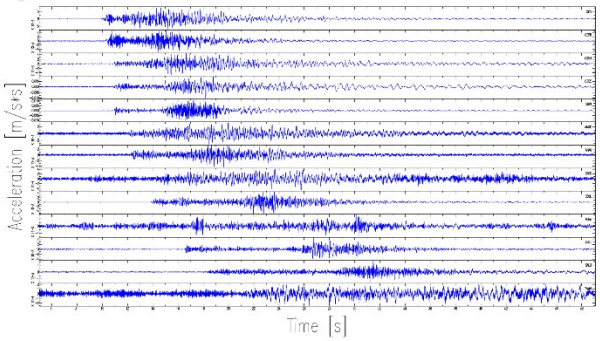

c)

SITE		Measured Parameters				Output of the system					
Name	Dist(Km)	Pd(cm)	Pv (cm/s)	Pa(cm/s^2)	TM check	PGA_Pd %g	PGA_Pv %g	PGA_Pa %g	PGA_comb %g	PGA_obs %g	EVENT TYPE
GIOV	29.8	0.000592	0.01674	0.7646	PASS	0.2167	0.2358	0.3146	0.2646	0.133	A1
CEPR	31.5	0.001181	0.01106	0.3046	PASS	0.1955	0.1649	0.1435	0.1603	0.0381	A1
CECC	35.7	0.000895	0.01259	0.6055	PASS	0.1595	0.1843	0.2578	0.2087	0.1348	A1
SUPI	36.6	0.000426	0.01242	0.935	PASS	0.1626	0.1821	0.3735	0.2477	0.1575	A1
ANAG	45.4	0.000287	0.00485	0.2458	PASS	0.115	0.0809	0.1195	0.1043	0.0608	A1
COLL	55.4	0.000116	0.00358	0.2644	PASS	0.0524	0.0621	0.1272	0.0834	0.0942	A1
LABI	66.6	0.000125	0.00408	0.1707	PASS	0.0558	0.0696	0.0876	0.0739	0.0525	A1
GALL	73.4	7.6e-05	0.00374	0.2429	PASS	0.0362	0.0646	0.1183	0.0756	0.0741	A1

Fig. S8.

Example of Real-time performance of the ALpEW system. a) position (with respect to the network infrastructure) of the largest recorded event with magnitude ML 3.4 on 2021-06-22 at 18:37:04 (http://terremoti.ingv.it/event/27189251), b) recorded waveforms in acceleration; c) summary of the performance of the EW system in terms of parameter estimates, Decision Module and Alert Declaration. Last column shows the "Event Type" as it was classified by the system. "A1" means that the system detected the transient signal, recognized that it was associated to the arrival of the P-wave produced by the earthquake, but it predicted that the expected PGA was not relevant enough to trigger the alert. Panel a) was obtained using Google Earth (web version 10.82.0.1 Multi-threaded, available at GoogleEarth, © Google Earth 2025).

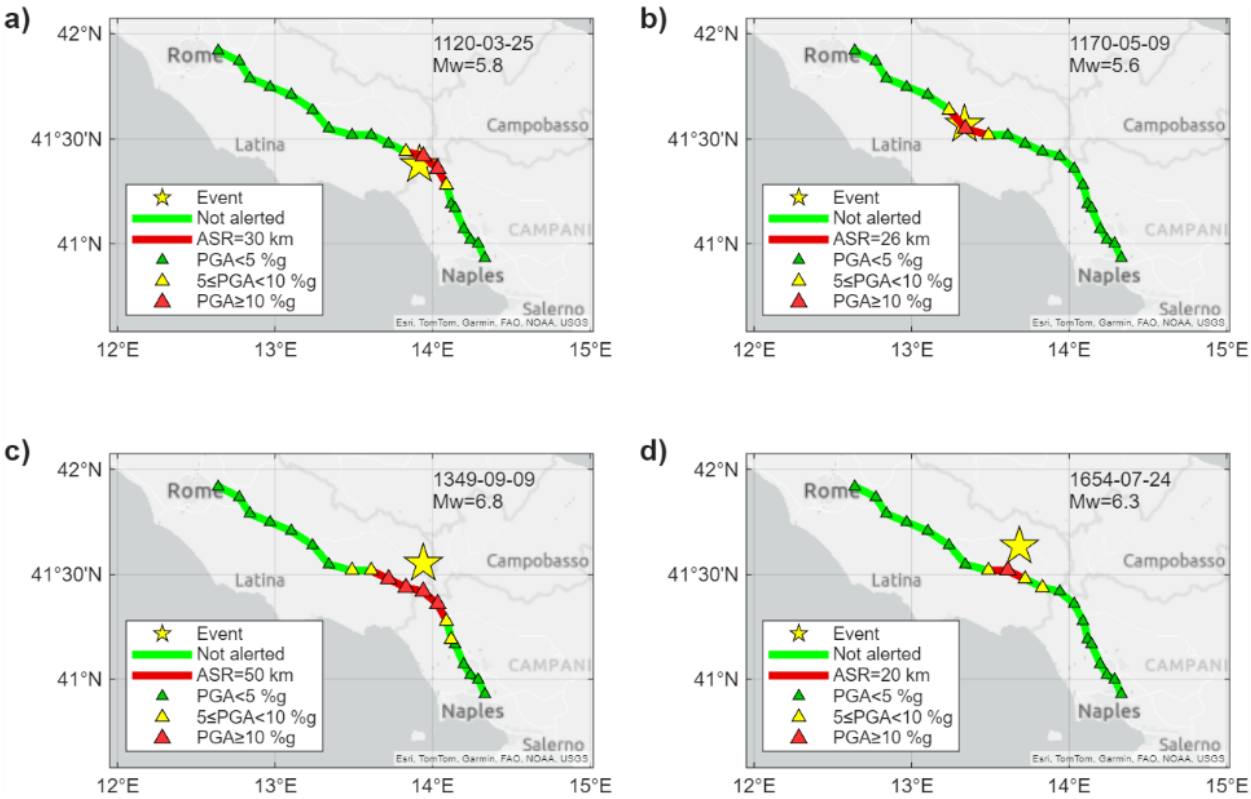

Figure S9.
Historical earthquake scenarios. The figure shows the predicted ASR in case of four different scenario earthquakes, occurred nearby the railway line and that would produce a PGA > 10 %g at least in one point along the railway, according to the region-specific GMPE. In all panels, the date and magnitude of the reference historical earthquake is reported in the top right corner; the yellow star is the earthquake epicenter and the colored triangles are the stations. The railway line is colored according to the predicted PGA values. The red portion of the line represented the Alerted Segment of the railway (ASR), while the green portion is the line in which no damage is expected, and the train circulation is allowed.

Table S1. Calibration parameters for the Train Marker Algorithm						
Station	**α**	**β**	**γ**	**TM Threshold**	**# trains training**	**# trains test**
AFRA	0.83	0.14	0.03	3.26	NA	NA
ANAG	0.330000	0.330000	0.340000	2.142235	5585	2393
ANGE	0.330000	0.340000	0.330000	2.132495	6985	2993
CASE	0.570000	0.310000	0.120000	2.630770	5829	2497
CASN	0.780000	0.060000	0.160000	3.238976	2413	1034
CASS	0.330000	0.330000	0.340000	2.142235	5675	2431
CECC	0.810000	0.000000	0.190000	3.348079	3048	1306
CEPR	0.330000	0.330000	0.340000	2.142235	5645	2419
COLL	0.330000	0.330000	0.340000	2.142235	8557	3667
GALL	0.330000	0.330000	0.340000	2.142235	5756	2466
GIOV	0.330000	0.330000	0.340000	2.142235	5572	2387
GRIC	0.530000	0.450000	0.020000	2.451185	7797	3341
LABI	0.650000	0.350000	0.000000	2.748817	7148	3063
MARC	0.330000	0.340000	0.330000	2.132495	196	84
PIGN	0.760000	0.240000	0.000000	3.053642	27805	11916
SALO	0.330000	0.330000	0.340000	2.142235	1980	848
SUPI	0.800000	0.040000	0.160000	3.291771	5536	2372
TAMM	0.990000	0.010000	0.000000	3.685616	6911	2961
TORA	0.330000	0.340000	0.330000	2.132495	6794	2911
VAIR	0.330000	0.330000	0.340000	2.142235	927	396

Table S1.

Calibration parameters for the TM algorithm. The table reports the α, β and γ coefficients and the threshold value on the TM parameter, as estimated for each station (PT). The coefficients are computed by fixing the percentage of missed events (corresponding to 3%) and then by minimizing the overlap between TM values for trains and earthquakes separately. The number of trains used during the training and testing phases is also reported in the last two columns.

Table S2: PGV-Px Regression Relationships			
1sec: PGA vs Px	**A**	**B**	**SE**
Pd	2.81 ($\pm$0.13)	0.73 ($\pm$0.05)	0.39
Pv	2.12 ($\pm$0.04)	0.79 ($\pm$0.02)	0.43
Pa	0.88 ($\pm$0.02)	0.70 ($\pm$0.02)	0.43
2sec: PGA vs Px	**A**	**B**	**SE**
Pd	2.74 ($\pm$0.09)	0.76 ($\pm$0.04)	0.42
Pv	2.11 ($\pm$0.03)	0.86 ($\pm$0.02)	0.38
Pa	0.75 ($\pm$0.01)	0.79 ($\pm$0.02)	0.36
3sec: PGA vs Px	**A**	**B**	**SE**
Pd	2.68 ($\pm$0.07)	0.77 ($\pm$0.03)	0.41
Pv	2.03 ($\pm$0.03)	0.88 ($\pm$0.02)	0.33
Pa	0.66 ($\pm$0.01)	0.84 ($\pm$0.02)	0.30
4sec: PGA vs Px	**A**	**B**	**SE**
Pd	2.56 ($\pm$0.06)	0.76 ($\pm$0.02)	0.40
Pv	1.95 ($\pm$0.03)	0.88 ($\pm$0.02)	0.33
Pa	0.61 ($\pm$0.01)	0.85 ($\pm$0.02)	0.28
5sec: PGA vs Px	**A**	**B**	**SE**
Pd	2.40 ($\pm$0.05)	0.73 ($\pm$0.02)	0.40
Pv	1.87 ($\pm$0.02)	0.86 ($\pm$0.01)	0.32
Pa	0.56 ($\pm$0.01)	0.85 ($\pm$0.01)	0.27

Table S2.

PGV-Px Regression Relationships. The table contains the A and B coefficients (and their uncertainties) for each empirical scaling relationship (from 1 to 5 sec) and the related standard error (last column).

Table S3: List of Decision Module combinations				
C_{index}	**DM**	**PGA (%g)**	**PGA_{inf} (%g)**	**EPL%**
1	SSBA	4%	-	50%
2	SSBA	4%	-	90%
3	SSBA	8%	-	50%
4	SSBA	8%	-	90%
5	SSBA	15%	-	50%
6	SSBA	15%	-	90%
7	SSRA1	4%	1%	50%
8	SSRA1	4%	1%	90%
9	SSRA1	4%	2%	50%
10	SSRA1	4%	2%	90%
11	SSRA1	8%	2%	50%
12	SSRA1	8%	2%	90%
13	SSRA1	10%	2%	50%
14	SSRA1	10%	2%	90%
15	SSRA2	4%	1%	50%
16	SSRA2	4%	1%	90%
17	SSRA2	4%	2%	50%
18	SSRA2	4%	2%	90%
19	MSA2	8%	-	50%
20	MSA2	8%	-	90%
21	MSA2	15%	-	50%
22	MSA2	15%	-	90%

Table S3.

List of combinations of the Decision Module for the performance evaluation. The table contains the list of all the combinations used to evaluate the performance of the system. From left to right, the Table shows the configuration in terms of Decision Module (DM), Threshold value of PGA and Exceedance Probability Level. In the case of the *SSR* configurations, the lower PGA threshold (PGA^{th}_{min}) for the adjacent nodes is set to 5% of g.

Reference List

Bindi, D., Pacor, F., Luzi, L., Puglia, R., Massa, M., Ameri, G., & Paolucci, R. (2011). Ground motion prediction equations derived from the Italian strong motion database. *Bulletin of Earthquake Engineering 2011 9:6*, *9*(6), 1899–1920. https://doi.org/10.1007/S10518-011-9313-Z

Peterson, J. R. (1993). Observations and modeling of seismic background noise. *Open-File Report*. https://doi.org/10.3133/OFR93322

Rovida, A., Locati, M., Camassi, R., Lolli, B., & Gasperini, P. (2020). The Italian earthquake catalogue CPTI15. Bulletin of Earthquake Engineering, 18(7), 2953-2984.